Research Article

HOTTIP downregulation reduces neuronal damage and microglial activation in Parkinson's disease cell and mouse models

https://doi.org/10.4103/1673-5374.322475

Date of submission: August 26, 2020

Date of decision: October 26, 2020

Date of acceptance: May 18, 2021

Date of web publication: August 30, 2021

Peng Lun[1, #], Tao Ji[2, #], De-Hong Wan[1], Xia Liu[3], Xiao-Dong Chen[4], Shuai Yu[4], Peng Sun[1, *]

Graphical Abstract *HOTTIP functions as a ceRNA by sponging miR-615-3p and promotes FOXO1 expression, which activates NF-κB and NLRP3 inflammasome, thereby aggravating inflammatory response and neuronal apoptosis in Parkinson's disease*

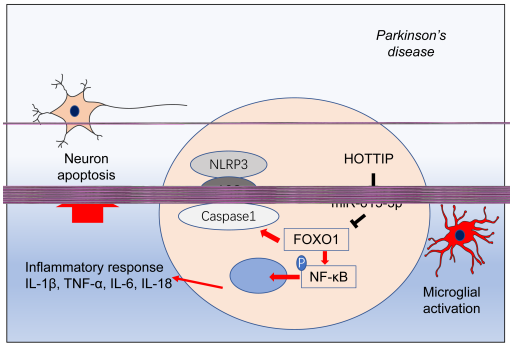

Abstract

HOXA transcript at the distal tip (HOTTIP), a newly identified long noncoding RNA, has been shown to exhibit anti-inflammatory effects and inhibit oxygen-glucose deprivation-induced neuronal apoptosis. However, its role in Parkinson's disease (PD) remains unclear. 1-Methyl-4-phenylpyridium (MPP^+) and 1-methyl-4-phenyl-1,2,3,6-tetrahydropyridine (MPTP) were used to establish PD models in SH-SY5Y and BV2 cells and in C57BL/6 male mice, respectively. *In vitro*, after HOTTIP knockdown by sh-HOTTIP transfection, HOTTIP and FOXO1 overexpression promoted SH-SY5Y apoptosis, BV2 microglial activation, proinflammatory cytokine expression, and nuclear factor kappa-B and NACHT, LRR and PYD domains-containing protein 3 inflammasome activation. Overexpression of miR-615-3p inhibited MPP^+-induced neuronal apoptosis and microglial inflammation and ameliorated HOTTIP- and FOXO1-mediated nerve injury and inflammation. *In vivo*, HOTTIP knockdown alleviated motor dysfunction in PD mice and reduced neuronal apoptosis and microglial activation in the substantia nigra. These findings suggest that inhibition of HOTTIP mitigates neuronal apoptosis and microglial activation in PD models by modulating miR-615-3p/FOXO1. This study was approved by the Ethics Review Committee of the Affiliated Hospital of Qingdao University, China (approval No. UDX-2018-042) in June 2018.

Key Words: apoptosis; inflammation; miR-615-3p; neuron; NLRP3; noncoding RNA; Parkinson's disease; HOTTIP

Chinese Library Classification No. R456; R741.05; R363

Introduction

Parkinson's disease (PD) is characterized by progressive degeneration and apoptosis of dopaminergic neurons and the appearance of Lewy bodies in the substantia nigra (SN), which causes neuron loss, static tremors, myotonia, bradykinesia, and abnormal posture and gait (Wakabayashi et al., 2013; Schneider et al., 2017). Recent studies have shown that inflammation and immune response contribute to dopaminergic neuron apoptosis. Neuroinflammation-mediated neurotoxicity contributes to the neuronal death cascade in PD patients (Rocha et al., 2018; Surmeier, 2018). Therefore, exploring inflammation in PD is vital to better understand the disorder in efforts to improve its diagnosis and treatment.

Microglia account for only 10% of central nervous system (CNS) cells, but exert a vital role in the modulation of neuroinflammation involved in CNS diseases (Xiong et al., 2016). Multiple agents, including 1-methyl-4-phenyl-1,2,3,6-tetrahydropyridine (MPTP), paraquat, rotenone, pathogen-associated molecular patterns, α-synuclein, matrix metalloproteinase 3, thrombin, and neuromelanin can activate microglia (Frank-Cannon et al., 2009). When microglia are activated, they produce oxygen-free radicals and toxic inflammatory mediators, which cause neuroinflammation through different molecular mechanisms, exacerbate dopaminergic nerve damage, and accelerate PD-induced neuroinflammation and neuronal death (Vivekanantham et al.,

[1]Department of Neurosurgery, the Affiliated Hospital of Qingdao University, Qingdao, Shandong Province, China; [2]Department of Neurosurgery, Laiyang People's Hospital, Yantai, Shandong Province, China; [3]Department of Endocrine and Metabolic Diseases, the Affiliated Hospital of Qingdao University, Qingdao, Shandong Province, China; [4]Emergency Department, the Affiliated Hospital of Qingdao University, Qingdao, Shandong Province, China

***Correspondence to:** Peng Sun, MD, PhD, pqhhu25@163.com.

https://orcid.org/0000-0001-8902-6925 (Peng Sun)

#Both authors contributed equally to this work.

How to cite this article: *Lun P, Ji T, Wan DH, Liu X, Chen XD, Yu S, Sun P (2022) HOTTIP downregulation reduces neuronal damage and microglial activation in Parkinson's disease cell and mouse models. Neural Regen Res 17(4):887-897.*

2015; Guo et al., 2019).

Long noncoding RNAs (lncRNAs) are a kind of RNA without the protein-coding ability and have a transcript length of over 200 nucleotides (Liu et al., 2020a). It has been shown that lncRNAs contribute to cell proliferation, differentiation, and death (Charles Richard and Eichhorn, 2018). They are abnormally expressed in multiple CNS diseases and exert a significant role by regulating microglia-mediated inflammation (Wang and Zhou, 2018; Zhang et al., 2019b). Additionally, lncRNAs have been shown to play a role in PD (Lin et al., 2019; Xu et al., 2020). HOXA transcript at the distal tip (HOTTIP) is a lncRNA involved in CNS disease. For example, HOTTIP expression was decreased in experimental ischemic stroke models, and HOTTIP overexpression relieves oxygen-glucose deprivation-induced neuronal apoptosis (Wang et al., 2018b). However, its function in PD deserves further study.

Like lncRNAs, microRNAs (miRNAs) are another type of noncoding single-stranded RNA with a length of about 20–24 nucleotides. MiRNAs regulate genes by combining with the 3′-untranslated region of a target gene and are involved in multiple diseases (Karthikeyan et al., 2016; Zhong et al., 2018). Multiple miRNAs have been found to regulate neuronal damage and microglial inflammation in PD (Brites and Fernandes, 2015; Prasad, 2017; Neal and Richardson, 2018). In particular, miR-615-3p is involved in multiple diseases, including cancer (Pu et al., 2017) and Huntington's disease (Hoss et al., 2014). Interestingly, HOTTIP targets miR-615-3p and facilitates hypoxia-induced glycolysis in non-small cell lung cancer (Wang et al., 2018a). Nevertheless, the impact of HOTTIP on miR-615-3p in PD remains unknown.

The coding gene of forkhead box protein O1 (FOXO1) is a member of the FOX transcription factor family that has a distinct forkhead domain (Rudd et al., 2007). Recent research suggests that FOXO1 functions as a gene regulator contributing to biological processes, such as longevity, protein turnover, substrate metabolism, cell survival, and cell death (Xing et al., 2018). For instance, the G-protein-coupled receptor, protease-activated receptor 2, can enhance the M1 polarization of macrophages through FOXO1, thereby exacerbating inflammation (Chen et al., 2019). Interestingly, FOXO1 is reversely modulated by miR-615-3p, thereby modulating osteogenic differentiation of human lumbar ligamentum flavum cells (Yin et al., 2017). Still, the function of miR-615-3p on FOXO1 in microglia-mediated neuroinflammation and its upstream mechanism in PD needs further study.

Thus, we hypothesized that both HOTTIP and miR-615-3p exert crucial functions in the mouse PD model and MPP^+-treated neurons and microglia. In this study, we constructed PD models with 1-methyl-4-phenylpyridium (MPP^+) and MPTP *in vitro* and *in vivo* to clarify the functions of HOTTIP and miR-615-3p in PD.

Materials and Methods

Experimental animals

The Ethics Review Board of the Affiliated Hospital of Qingdao University authorized this experiment (approval No. ZHQD2018-0322) in June 2018, and the experiment was implemented in accordance with the instructions for the feeding, management and utilization of experimental animals formulated by the National Institutes of Health. Forty-eight C57BL/6 male mice (20–22 g, 8–10 weeks old, specific-pathogen-free level) were bought from the Animal Center of Shandong University (license No. SCXK (Lu) 2019 0001) and raised in sterile equipment (25 ± 2°C, with the relative humidity of 60–70%) with a 12 hour light/12 hour dark cycle. The mice could eat and drink freely, and they were randomized into four groups: sham, MPTP, MPTP + sh-NC, and MPTP + sh-HOTTIP, with 12 mice in each group.

The PD model was established through intraperitoneal injection of MPTP-HCl (20 mg/kg; MilliporeSigma, St. Louis, MO, USA). An equal amount (200 μL) of normal saline was injected into mice in the Sham group. The MPTP + sh-HOTTIP group was injected with lentivirus sh-HOTTIP (Ruibo Biotechnology Co., Ltd., Guangzhou, China) and the MPTP + sh-NC group was injected with its negative control (sh-NC). The mice were injected with the lentiviral sh-HOTTIP vector or sh-NC via the right ventricle (bregma: –2 mm, lateral: 2 mm, dorsoventral: 3 mm; Paxinos and Watson, 2007) using a stereotactic catheter (Stoelting Co., Wood Dale, IL, USA); 5 μL solvent containing 20 nM sh-HOTTIP or sh-NC was injected via a catheter every day for five consecutive days. The intraperitoneal administration of MPTP began 24 hours after the last injection of the solvent. All surgical operations were implemented under anesthesia with 40 mg/kg phenobarbital sodium (Standardpharm Co. Ltd., New York, NY, USA) via intraperitoneal injection. Neurological behaviors of the mice were evaluated during the 56 days following MPTP administration. The mice were sacrificed after they were deeply anesthetized by intraperitoneal injection of phenobarbital sodium (150 mg/kg) on day 57 for sampling.

Cell culture

Neuroblastoma SH-SY5Y cells and BV2 microglial cells were bought from the Cell Center of the Chinese Academy of Sciences (Shanghai, China). Afterward, they were cultured in the Dulbecco's modified Eagle medium (Thermo Fisher HyClone, Logan, UT, USA) containing 10% fetal bovine serum (Invitrogen, Carlsbad, CA, USA) and 1% penicillin/streptomycin (Invitrogen) and incubated at 37°C with 5% CO_2. The Dulbecco's modified Eagle medium and fetal bovine serum were from Thermo Fisher Scientific. During the logarithmic growth phase of the cells, 0.25% trypsin (Thermo Fisher HyClone) was used for trypsinization and subculture.

SH-SY5Y and BV2 cells in the logarithmic growth phase were cultured in 96-, 24-, or 6-well plates. After cell growth was stable, different doses of MPP^+ (12.5–100 μM; Millipore Sigma) were added for 24 hours.

Cell transfection

PcDNA empty vector (NC), pcDNA3.1-HOTTIP (HOTTIP), miRNA control (miR-NC), and miR-615-3p mimics were bought from GenePharma Co., Ltd. (Shanghai, China). SH-SY5Y and BV2 cells were seeded in 24-well plates at 3×10^5/well, incubated at 37°C with 5% CO_2 for 24 hours, and then transfected. Afterward, the above vectors (50 nM) and Lipofectamine® 3000 (Invitrogen) were mixed and co-transfected into SH-SY5Y and BV2 as per the supplier's guidelines. After 24 hours, the original medium was discarded, fresh medium was provided, and the cells were further cultured for 24 hours. Finally, reverse transcription-polymerase chain reaction (RT-PCR) was applied to test the transfection validity.

Cell viability test

SH-SY5Y cells transfected with pcDNA3.1-HOTTIP and/or miR-615-3p mimics were obtained, and the suspension was seeded into 96-well plates (100 μL/well at 5×10^4 cells/mL). Then, the plates were put in an incubator for preculture (37°C, 5% CO_2). After the cells were treated with MPP^+ (12.5–100 μM; MilliporeSigma), each well was supplemented with 10 μL Cell Counting Kit-8 solution (Beyotime, Shanghai, China) and incubated for 1 hour. The optical density was determined at 450 nm using a Thermo Scientific Microplate Reader (Waltham, MA, USA).

Flow cytometry

SH-SY5Y cells transfected with pcDNA3.1-HOTTIP and/or miR-615-3p mimics were collected, and the cell suspension (2000 μL/well, 1×10^5 cells/mL) was inoculated in 6-well

plates. After the cells were treated with MPP^+ (12.5–100 μM; MilliporeSigma), the cells were processed with ethylenediaminetetraacetic acid-free trypsin and collected. Then, they were cleared twice with precooled phosphate-buffered saline (PBS), and 1–5 × 10^5 cells were harvested. Afterward, 100 μL 1× binding buffer was added for cell resuspension, and 5 μL AnnexinV-fluorescein isothiocyanate and 5 μL propidium iodide staining solution (Solarbio, Beijing, China) was supplemented, mixed gently in the dark, and incubated at room temperature for 10 minutes. Subsequently, 400 μL 1× binding buffer was supplemented and mixed well. The apoptotic level was examined with FACScan flow cytometry (BD Biosciences, Franklin Lakes, NJ, USA) within 1 hour.

Dual-luciferase reporter gene assay

The online database Starbase (http://starbase.sysu.edu.cn/) was used to predict the potential miRNA targets of HOTTIP and FOXO1. On the basis of the analysis, the wild-type (wt) reporter vectors HOTTIP-wt and FOXO1-wt containing the luciferase vector, and reporting vectors HOTTIP-mut and FOXO1-mut that were mutated at the miR-615-3p binding site, were acquired from GenePharma. SH-SY5Y and BV2 cells were seeded in 24-well plates (1000 μL/well at 5 × 10^5 cells/mL). After the cells cultured overnight until the fusion rate reached 70%, miR-615-3p mimics and miR-NC were co-transfected with HOTTIP-wt, FOXO1-wt, HOTTIP-mut and FOXO1-mut. After cell lysis, the dual-luciferase reporter system (RiboBio, Guangzhou, China) was used to determine the luciferase activity of the samples.

RT-PCR

The RNA from nuclear and cytoplasmic fractions from SH-SY5Y and BV2 cells was isolated using the PARIS kit (Cat# AM1921; Thermo Fisher Scientific, Yokohama, Japan) according to the manufacturer's instructions. Briefly, SH-SY5Y and BV2 cells were collected and washed with PBS three times. Next, the precooled cell fractionation buffer (300 μL) was used to resuspend the cells, which were then incubated on ice for 10 minutes. After that, the cells were collected and centrifuged (500 × *g*) for 5 minutes. The supernatant containing the cytoplasmic fraction was collected, leaving behind the nucleus-rich pellet. Nuclear and cytoplasmic RNA were then precipitated after elution at room temperature. The relative expression of *Hottip* and *miR-615-3p* were determined by real time quantitative PCR (RT-qPCR). *U6* and *GAPDH* served as internal control transcripts for nuclear and cytoplasmic RNA, respectively.

Total RNA was separated from tissues or cells with the TRIzol reagent (Invitrogen). The PrimeScript™ RT Reagent kit (Invitrogen (China), Shanghai, China) was used to reverse-transcribe the RNA into complementary DNA after the content and purity determination. The qPCR was carried out with the Bio-Rad CFX96 quantitative PCR system and the SYBR green PCR mixture. PCR was performed with predenaturation at 95°C for 5 minutes, denaturation at 95°C for 15 seconds, and annealing at 60°C for 30 seconds. *U6* served as the internal reference for *miR-615-3p*, and *GAPDH* and *U6* served as the internal references for the remaining molecules. The $2^{-\Delta\Delta Ct}$ was used for statistical analysis. Each test was conducted in triplicate. The specific primer sequences were shown in **Table 1**.

Western blot assay

The Bradford method was used for protein extraction and quantification. Protein from SH-SY5Y and BV2 cells and samples from SN area in PD mice was boiled for 5 minutes, cooled on ice, and centrifuged for 30 seconds. Afterward, the supernatant was collected for polyacrylamide gel electrophoresis and transferred to polyvinylidene fluoride membranes at 100 V for 1 hour. Next, the membranes were blocked with 5% skim milk at room temperature for 1 hour and then incubated with the primary rabbit anti-Caspase-3 antibody (Cat# ab13847, 1:1000), recombinant rabbit anti-Bax antibody (Cat# ab32503, 1:1000), recombinant rabbit anti-Bcl-2 antibody (Cat# ab32124, 1:1000), mouse anti-β-actin antibody (Cat# ab6276, 1:2000), recombinant rabbit anti-NACHT, LRR and PYD domains-containing protein 3 (NLRP3) antibody (Cat#ab263899, 1:1000), rabbit anti-Caspase-1 antibody (Cat# ab207802, 1:1000), recombinant rabbit anti-adaptor protein apoptosis-associated speck-like protein containing a CARD (ASC) antibody (Cat# ab151700, 1:1000), rabbit anti-inducible nitric oxide synthase (iNOS) antibody (Cat# ab178945, 1:1000), rabbit anti-cyclooxygenase 2 (COX2) antibody (Cat# ab179800, 1:1000), rabbit anti-nuclear factor kappa-B (NF-κB) p65 antibody (Cat# ab16502, 1:1000), rabbit anti-NF-κB p65 (phospho S529) antibody (Cat# ab109458, 1:1000), rabbit anti-FOXO1 antibody (Cat# ab52857, 1:1000), rabbit anti-histone H3 antibody (Cat# ab215728, 1:1000), rabbit anti-tyrosine hydroxylase (TH) antibody (neuronal marker; Cat# ab112, 1:1000) and recombinant rabbit anti-ionized calcium-binding adapter molecule 1 (Iba1) antibody (Cat# ab178846, 1:1000) (all purchased from Abcam, Cambridge, MA, USA) overnight at 4°C. After that, the membranes were cleared with Tris buffered saline solution containing 0.1% Tween 20 twice and incubated with the goat anti-rabbit or goat anti-mouse horseradish peroxidase-labeled secondary antibodies (Cat# ab205718, 1:2000, Abcam) at room temperature for 1 hour. The membranes were cleared three times before being exposed to electro-chemiluminescence luminescence reagent (Thermo Fisher HyClone), and the membrane scanner (Bio-Rad, Hercules, CA, USA) was used for imaging.

Table 1 | **Primers used in this study**

Gene	Forward primer (5'–3')	Reverse primer (5'–3')
Hottip	CCT AAA GCC ACG CTT CTT TG	TGC AGG CTG GAG ATC CTA CT
miR-615-3p	ACA CTC CAG CTG GGT CCG AGC CTG GGT CTC	TGG TGT CGT GGA GTC
Foxo1	TTT CTA AGT GGC CTG CGA GT	GGT GGA TAC ACC AGG GAA TG
β-Actin	TGA GAG GGA AAT CGT GCG TG	TTG CTG ATC CAC ATC TGC TGG
U6	CTC GCT TCG GCA GCA CAT ATA CT	ACG CTT CAC GAA TTT GCG TGT C

Enzyme linked immunosorbent assay

The enzyme linked immunosorbent assay (ELISA) kit from Multisciences (Lianke) Biotech, Co., Ltd. (Hangzhou, China) was used to measure interleukin (IL)-lβ, IL-6, IL-18, and tumor necrosis factor (TNF)-α levels in BV2 cells according to the kit instructions using a Thermo Scientific Microplate Reader.

Immunohistochemistry

The brains from mice in each group were paraffin-embedded, sectioned (4 μm), dewaxed, and then repaired under high pressure with a 0.01 mM sodium citrate buffer solution for 15 minutes. After natural cooling, the sections were washed with 1× PBS three times (3 minutes each time). Then, 3 mL/L H_2O_2 was added and the sections were incubated in a humid box for 10 minutes to inactivate the endogenous peroxidase. Subsequently, the sections were rinsed with 1× PBS three times (3 minutes each time), and then incubated with the rabbit anti-TH antibody (Cat# ab112, 1:150, Abcam), rabbit anti-Iba1 (Cat# ab178846, 1:100, Abcam) and rabbit anti-Caspase-3 antibody (Cat# ab13847, 1:200, Abcam) at 4°C overnight. Next, they were rinsed with 1× PBS three times (5 minutes each time) and incubated with the horseradish peroxidase-goat anti-rabbit IgG (H&L) (Cat# ab205718, 1:200 Abcam) at room temperature for 30 minutes. After being rinsed with 1× PBS three times (5 minutes per time), the sections were developed with 3,3′-diaminobenzidine tetrahydrochloride for 3 minutes, counterstained with hematoxylin and eosin staining, mounted, observed with

a light microscope (CX31, Olympus, Tokyo, Japan), and photographed. The Image-Pro Plus 6.0 software (National Institutes of Health, Bethesda, MD, USA) was used for quantitative analysis.

Neurological function evaluation

The motor function of the mice was evaluated by the Rotarod test (Luo et al., 2018). Mice were placed on an accelerating rod (Unibiolab, Beijing, China). The rotation speed gradually increased from 2 r/min to 20 r/min. The time to the mouse's first fall was recorded, with a maximum of 300 seconds. The test was implemented every 14 days for 56 days.

Latency to fall and grip strength were measured to assess the muscular forelimb strength on day 56 after surgery with the inverted screen test and forelimb grip strength test, respectively (Singh et al., 2017). The mouse was put in the center of a wire mesh screen (Shanghai Yuyan Scientific Instrument Co., Ltd., Shanghai, China) and then rotated upside down. Latency to fall was measured in seconds. A grip strength tester (Shanghai Yuyan Scientific Instrument Co., Ltd.) was used to test muscular forelimb strength.

The pole test was conducted to assess bradykinesia (Lee et al., 2019). Mice were placed on top of a 55-cm-high rough pole (8 mm in diameter). We recorded how long it took the mice to turn completely around, climb down and reach the ground with four paws. Each trial had a maximum length of 30 seconds.

Dopamine content measurements

High performance liquid chromatography (HPLC) was used to measure dopamine content in the striatal area of mice according to a previous study (Yang et al., 2014). Briefly, the brain tissue of the striatal area was isolated, weighed, dissected, homogenized and lysed in 400 μL of ice-cold 0.1 M perchloric acid for 10 minutes. After that, the homogenates were centrifuged (14,000 × *g*, 10 minutes) at 4°C. The supernatant was collected and then subjected to the HPLC (Nexera UHPLC/HPLC System, Shimadzu, Japan) for dopamine content determination. Empower software (Waters Corporation, Milford, MA, USA) was used for data analysis. Dopamine content was quantified in reference to an external standard.

Statistical analysis

The data were analyzed with SPSS 22.0 statistical software (IBM, Armonk, NY, USA). The data are presented as mean ± standard deviation (SD). Pairwise comparisons were made by Student's *t*-test, and comparisons between multiple groups were performed with one-way analysis of variance followed by Student-Newman-Keuls test. $P < 0.05$ represented statistical significance.

Results

MPP^+ treatment changes HOTTIP, miR-615-3p and FOXO1 expression

We treated SH-SY5Y and BV2 cells with different doses of MPP+ for 24 hours to investigate the role of HOTTIP, miR-615-3p and FOXO1 in PD. We conducted RT-PCR and western blot to measure HOTTIP, miR-615-3p and FOXO1 levels in the cells. MPP+ dose-dependently elevated HOTTIP expression and dampened miR-615-3p expression in SH-SY5Y and BV2 cells (**Figure 1A–D**). RT-PCR and western blot showed that the mRNA and protein expression of FOXO1 were elevated by MPP^+, and the elevation was enhanced with the increasing MPP^+ doses (**Figure 1E–H**). Thus, HOTTIP, miR-615-3p and FOXO1 were altered in MPP^+-treated SH-SY5Y and BV2 cells.

The function of HOTTIP and miR-615-3p in regulating MPP^+-induced neuronal toxicity

We transfected SH-SY5Y cells with vectors to overexpress HOTTIP, miR-615-3p, or both. Upregulating HOTTIP inhibited miR-615-3p, and upregulating miR-615-3p inhibited HOTTIP (**Figure 2A** and **B**). Next, the Cell Counting Kit-8 method and flow cytometry were used to examine cell viability and apoptosis, respectively. Compared with the control group, the HOTTIP group had reduced cell viability and increased cell apoptosis (**Figure 2C** and **D**). In contrast, miR-615-3p overexpression did not have a significant effect on cell viability and apoptosis. However, forced miR-615-3p overexpression in the HOTTIP group enhanced cell viability and reduced apoptosis ($P < 0.05$, *vs*. HOTTIP group; **Figure 2C** and **D**). Next, we treated SH-SY5Y cells with MPP^+ to investigate the effect of HOTTIP and miR-615-3p on neuronal toxicity in the MPP^+ PD cellular model. MPP^+ treatment significantly decreased SH-SY5Y viability ($P < 0.05$, *vs*. control group; **Figure 2E**) and increased the apoptosis rate ($P < 0.05$, *vs*. control group; **Figure 2F–G**). In addition, miR-615-3p overexpression enhanced SH-SY5Y cell viability and suppressed apoptosis compared with the MPP^+ group, whereas HOTTIP overexpression had the opposite effect, indicating that HOTTIP exacerbated the MPP^+-induced cellular damage ($P < 0.05$; **Figure 2E–G**). Interestingly, the MPP^+ + miR + lnc group had increased cell viability and decreased apoptosis compared with the MPP^+ + lnc group, suggesting that miR-615-3p alleviated HOTTIP-mediated cellular damage. Furthermore, we measured the expression of apoptosis-related proteins (cleaved Caspase-3, Bax, and Bcl2) and NLRP3-ASC-cleaved Caspase-1 inflammasomes with western blot. MPP^+ enhanced Caspase-3, Bax, and NLRP3-ASC-Caspase-1 inflammasome expression and suppressed Bcl2 expression (**Figure 2H** and **I**). miR-615-3p overexpression attenuated the proapoptotic proteins and NLRP3-ASC-Caspase-1 inflammasomes, whereas HOTTIP had the opposite effect (**Figure 2H** and **I**). The above results demonstrated that HOTTIP exacerbated the MPP^+-induced neuronal toxicity, and miR-615-3p attenuated the MPP^+-induced neuronal toxicity and weakened the effect of HOTTIP upregulation.

The function of HOTTIP and miR-615-3p in regulating MPP^+-induced microglial inflammation

Microglial activation is a key feature in PD (Vivekanantham et al., 2015). Therefore, we constructed HOTTIP and miR-615-3p overexpression models in BV2 cells. ELISA and western blot showed that the proinflammatory cytokines (including IL-lβ, IL-6, IL-18, and TNF-α), the pro-oxidant proteins iNOS and COX2, and the proinflammatory protein phosphorylated NF-κB produced by BV2 cells were upregulated after MPP+ treatment ($P < 0.05$; **Figure 3A–C**). Overexpression of miR-615-3p and HOTTIP suppressed and enhanced the above-mentioned inflammatory response, respectively ($P < 0.05$; **Figure 3A–C**). BV2 cells in the MPP^+ + miR + lnc group had a lower proinflammatory response than those in the MPP^+ + lnc group ($P < 0.05$; **Figure 3A–C**). Next, we measured the NLRP3-ASC-Caspase-1 inflammasome expression in BV2 cells. MPP^+ induced NLRP3-ASC-Caspase-1 inflammasome activation and miR-615-3p overexpression attenuated this effect (compared with the MPP^+ group). In contrast, HOTTIP overexpression enhanced the NLRP3-ASC-Caspase-1 inflammasome activation compared with the MPP^+ group ($P < 0.05$; **Figure 3D**). Moreover, miR-615-3p suppressed the HOTTIP-induced activation of NLRP3-ASC-Caspase-1 inflammasomes ($P < 0.05$; **Figure 3D**). These results suggest that HOTTIP was proinflammatory, whereas miR-615-3p was anti-inflammatory in MPP^+-induced inflammation.

Both HOTTIP and FOXO1 target miR-615-3p

The online database Starbase (http://starbase.sysu.edu.cn/) was used to predict the potential targets of HOTTIP and FOXO1. Starbase indicated that miR-615-3p binds to HOTTIP and FOXO1 (**Figure 4A** and **B**). Next, we compared the profiles of miR-615-3p, HOTTIP and FOXO1 in SH-SY5Y and BV2 cells under different treatments. Compared with the MPP^+ +

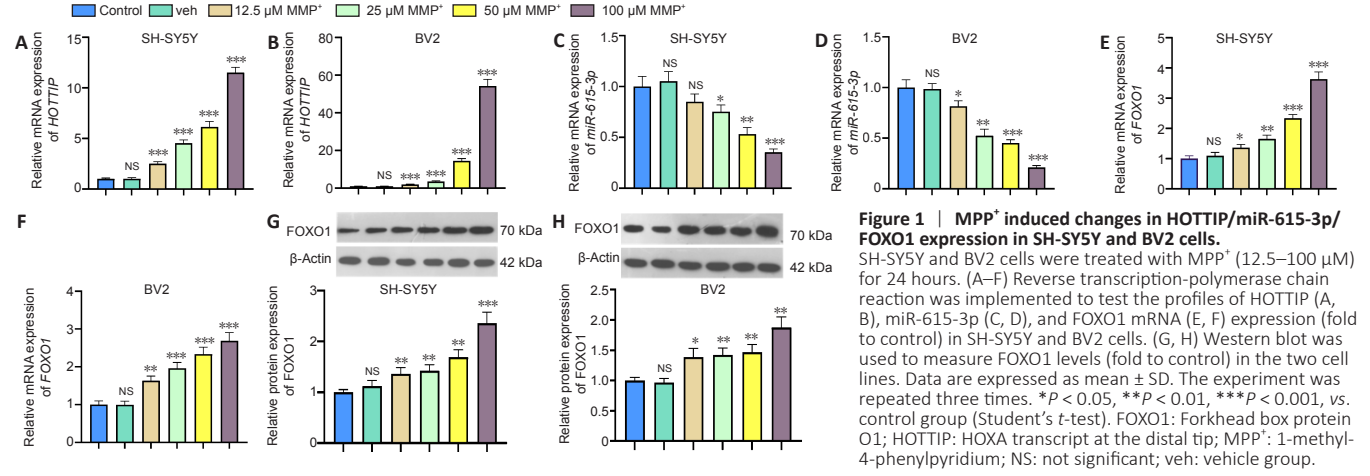

Figure 1 | MPP$^+$ induced changes in HOTTIP/miR-615-3p/FOXO1 expression in SH-SY5Y and BV2 cells.
SH-SY5Y and BV2 cells were treated with MPP$^+$ (12.5–100 μM) for 24 hours. (A–F) Reverse transcription-polymerase chain reaction was implemented to test the profiles of HOTTIP (A, B), miR-615-3p (C, D), and FOXO1 mRNA (E, F) expression (fold to control) in SH-SY5Y and BV2 cells. (G, H) Western blot was used to measure FOXO1 levels (fold to control) in the two cell lines. Data are expressed as mean ± SD. The experiment was repeated three times. *P < 0.05, **P < 0.01, ***P < 0.001, *vs.* control group (Student's *t*-test). FOXO1: Forkhead box protein O1; HOTTIP: HOXA transcript at the distal tip; MPP$^+$: 1-methyl-4-phenylpyridium; NS: not significant; veh: vehicle group.

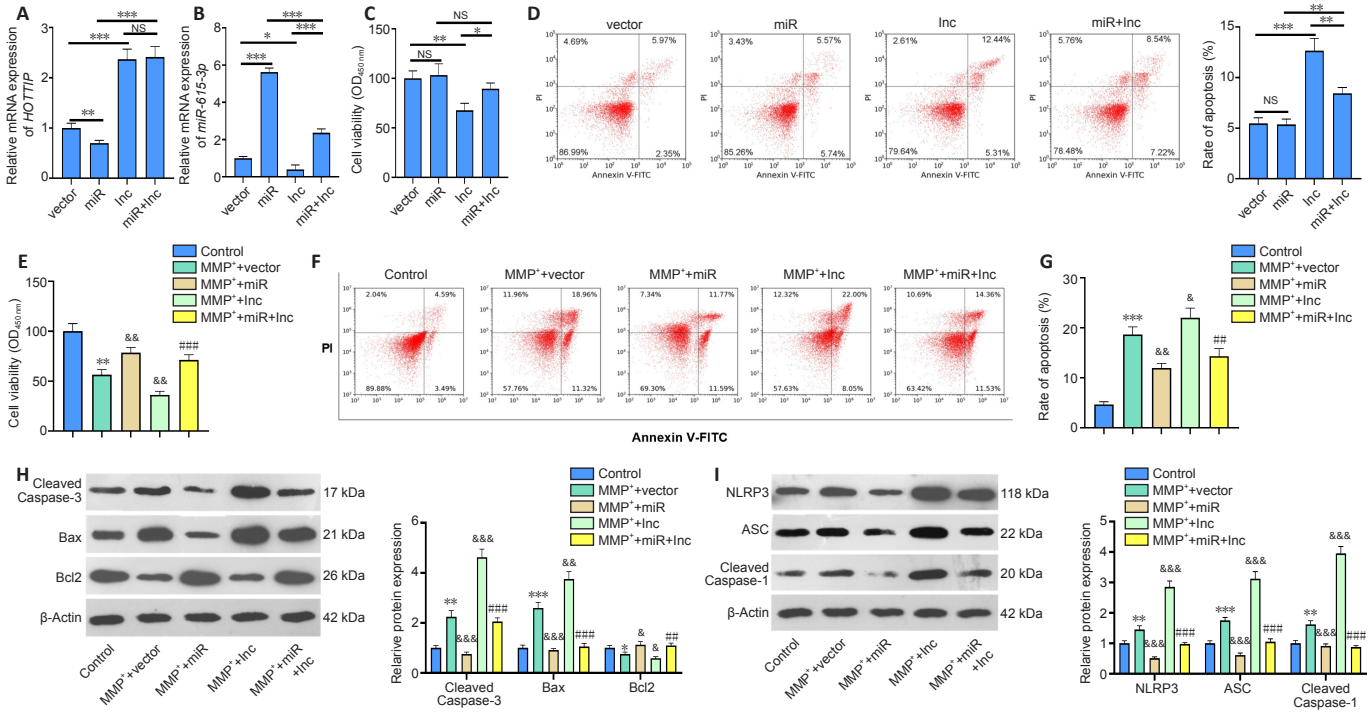

Figure 2 | The role of HOTTIP/miR-615-3p in regulating MPP$^+$-induced neuronal toxicity in SH-SY5Y cells.
(A–C) SH-SY5Y cells were transfected with HOTTIP/miR-615-3p overexpression vectors. (A, B) Reverse transcription-polymerase chain reaction was used to detect HOTTIP (A) and miR-615-3p (B) mRNA expression (fold to control). (C) CCK8 assay was used to determine cell viability. (D–I) SH-SY5Y cells transfected with HOTTIP/miR-615-3p overexpression vectors were treated with MPP$^+$ (100 μM) for 24 hours. (D) Cell apoptosis was monitored by flow cytometry. (E) CCK8 was used to determine cell viability. (F, G) Cell apoptosis was monitored by flow cytometry. The percentage of apoptotic cells is indicated by the numerical value represented in the upper right quadrant. (H, I) Western blot was used to measure the protein expression (fold to control) of cleaved Caspase-3, Bax and Bcl2, and NLRP3-ASC-cleaved Caspase-1 inflammasome. Data are expressed as mean ± SD. The experiment was repeated three times.*P < 0.05, **P < 0.01, *** P < 0.001, *vs.* control group; &P < 0.05, &&P < 0.01, &&&P < 0.001, *vs.* MPP$^+$ + vector group; ##P < 0.01, ###P < 0.001, *vs.* MPP$^+$ + lnc group (Student's *t*-test). ASC: Adaptor protein apoptosis-associated speck-like protein containing CARD domain; CCK8: Cell counting kit-8; HOTTIP: HOXA transcript at the distal tip; lnc: long non-coding; miR: microRNA; MPP$^+$: 1-methyl-4-phenylpyridium; NLRP3: NLR family pyrin domain containing 3; NS: not significant; OD: optical density.

vector group, the MPP$^+$ + lnc group had increased HOTTIP and FOXO1 levels, and decreased miR-615-3p levels (**Figure 4C–E**). In contrast, FOXO1 was downregulated, miR-615-3p was upregulated, and HOTTIP did not change significantly in the MPP$^+$ + lnc + miR group compared with the MMP$^+$ + lnc group (**Figure 4C–E**). Next, we implemented RT-PCR to examine the distribution of miR-615-3p and HOTTIP in SH-SY5Y and BV2 cells. Both HOTTIP and miR-615-3p were mainly distributed in the cytoplasm (**Figure 4F–G**). Furthermore, we carried out a dual-luciferase reporter assay to examine the association between HOTTIP and FOXO1. The miR-615-3p mimics markedly dampened the luciferase activity of cells transfected with HOTTIP-wt and FOXO1-wt (containing miR-615-3p binding sites), and had little impact on that of cells transfected with HOTTIP-mut and FOXO1-mut (containing mutated miR-615-3p binding sites) (**Figure 4H–I**). Thus, HOTTIP inhibited miR-615-3p, and the latter targeted the 3′-untranslated region of FOXO1 in SH-SY5Y and BV2 cells.

Overexpressing FOXO1 exacerbates the MPP$^+$-induced neuronal damage

We constructed a FOXO1 overexpression SH-SY5Y cell model to investigate the effect of FOXO1 on neurons in PD (**Figure 5A**). We transfected miR-615-3p into cells overexpressing FOXO1, and FOXO1 was suppressed in the MPP$^+$ + FOXO1 + miR group compared with that in the MPP$^+$ + FOXO1 group (P < 0.05; **Figure 5B**). Next, we tested the levels of neuronal viability and apoptosis. Cell viability and Bcl2 expression were suppressed, whereas cell apoptosis and Caspase-3 and Bax expressions were elevated in the MPP$^+$ + FOXO1 group compared with MPP$^+$ + vector group (P < 0.05; **Figure 5C–E**). In contrast, SH-SY5Y viability was enhanced and apoptosis was reduced in the MPP$^+$ + vector group compared with that of the MPP$^+$ + FOXO1 group (P < 0.05; **Figure 5C–E**). Subsequently, we measured the expression of NLRP3-ASC-Caspase-1 inflammasomes. FOXO1 overexpression facilitated the expression of NLRP3-ASC-Caspase-1, and this effect was attenuated by miR-615-3p

(**Figure 5F**). Thus, FOXO1 upregulation exacerbated the MPP^+-induced neuronal damage, possibly by activating NLRP3-ASC-Caspase-1 inflammasomes.

FOXO1 enhances MPP^+-induced inflammation in microglia

Next, we constructed a FOXO1 overexpression model in BV2 cells (**Figure 6A**) and showed that miR-615-3p overexpression suppressed FOXO1 expression (**Figure 6B**). Subsequently, we treated BV2 cells with MPP^+ and detected the expression of inflammatory factors and proteins by ELISA and western blot. IL-lβ, IL-6, IL-18, TNF-α, iNOS, COX2, and phosphorylated NF-κB were upregulated in the MPP^+ + FOXO1 group compared with the MPP^+ group ($P < 0.05$; **Figure 6C–E**). In contrast, miR-615-3p overexpression inhibited the above-mentioned inflammatory response ($P < 0.05$; **Figure 6C–E**). Finally, western blot was implemented to measure the expression of NLRP3-ASC-cleaved Caspase-1 inflammasomes. FOXO1 upregulation further activated the NLRP3-ASC-Caspase-1 inflammasome, and miR-615-3p overexpression dampened this effect ($P < 0.05$ *vs.* MPP^+ + FOXO1 group; **Figure 6F**). These results suggest that FOXO1 exerted a proinflammatory effect on MPP+-induced inflammation.

HOTTIP knockdown alleviates neurological dysfunction and neuronal damage in PD mice

We induced a PD mouse model combined with HOTTIP knockdown to explore the therapeutic effect of HOTTIP in MPTP-induced PD. First, we assessed the neurological changes in mice. Rotarod time and latency to fall were shorter, and grip strength and pole test scores were lower in PD mice than in sham mice ($P < 0.001$; **Figure 7A–D**). However, the neurological scores of HOTTIP knockdown PD mice were significantly improved compared with those of control PD mice ($P < 0.05$; **Figure 7A–D**).

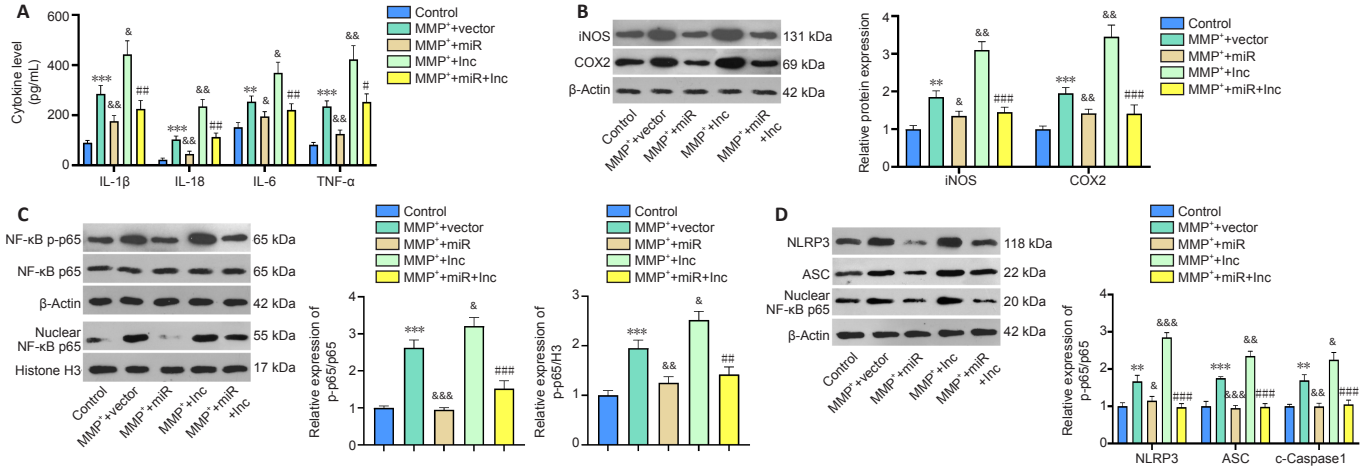

Figure 3 | The function of HOTTIP/miR-615-3p in regulating MPP^+-mediated inflammation in microglia (BV2 cells).
BV2 cells were transfected with a HOTTIP or miR-615-3p overexpression vector and then were treated with MPP^+ (100 μM) for 24 hours. (A) ELISA was performed to measure IL-lβ, IL-6, IL-18 and TNF-α levels produced by BV2 cells. (B–D) Western blot was used to measure the activation of pro-oxidant proteins iNOS and COX2 (B), proinflammatory protein phosphorylated NF-κB (C) and NLRP3-ASC-cleaved Caspase-1 inflammasome (D) (fold to control). Data are expressed as mean ± SD. The experiment was repeated three times. $^{**}P < 0.01$, $^{***}P < 0.001$, *vs.* control group; &$P < 0.05$, &&$P < 0.01$, &&&$P < 0.001$, *vs.* MPP^+ + vector group; #$P < 0.05$, ##$P < 0.01$, ###$P < 0.001$, *vs.* MPP^+ + lnc group (Student's *t*-test). ASC: Adaptor protein apoptosis-associated speck-like protein containing CARD domain; COX2: cyclooxygenase-2; ELISA: enzyme linked immunosorbent assay; HOTTIP: HOXA transcript at the distal tip; IL: interleukin; iNOS: inducible nitric oxide synthase; lnc: long non-coding; miR: microRNA; MPP^+: 1-methyl-4-phenylpyridium; NF-κB: nuclear factor kappa B; NLRP3: NLR family pyrin domain containing 3; TNF-α: tumor necrosis factor-α.

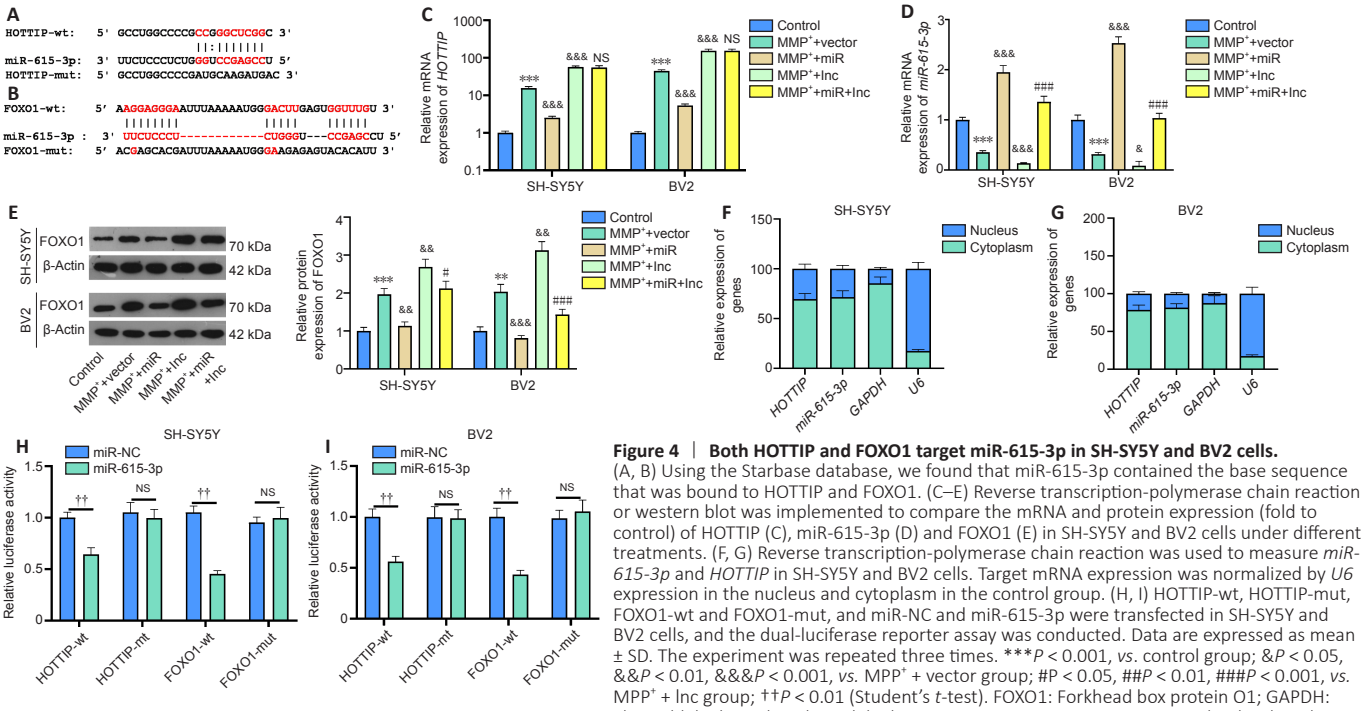

Figure 4 | Both HOTTIP and FOXO1 target miR-615-3p in SH-SY5Y and BV2 cells.
(A, B) Using the Starbase database, we found that miR-615-3p contained the base sequence that was bound to HOTTIP and FOXO1. (C–E) Reverse transcription-polymerase chain reaction or western blot was implemented to compare the mRNA and protein expression (fold to control) of HOTTIP (C), miR-615-3p (D) and FOXO1 (E) in SH-SY5Y and BV2 cells under different treatments. (F, G) Reverse transcription-polymerase chain reaction was used to measure *miR-615-3p* and *HOTTIP* in SH-SY5Y and BV2 cells. Target mRNA expression was normalized by *U6* expression in the nucleus and cytoplasm in the control group. (H, I) HOTTIP-wt, HOTTIP-mut, FOXO1-wt and FOXO1-mut, and miR-NC and miR-615-3p were transfected in SH-SY5Y and BV2 cells, and the dual-luciferase reporter assay was conducted. Data are expressed as mean ± SD. The experiment was repeated three times. $^{***}P < 0.001$, *vs.* control group; &$P < 0.05$, &&$P < 0.01$, &&&$P < 0.001$, *vs.* MPP^+ + vector group; #P < 0.05, ##$P < 0.01$, ###$P < 0.001$, *vs.* MPP^+ + lnc group; ††$P < 0.01$ (Student's *t*-test). FOXO1: Forkhead box protein O1; GAPDH: glyceraldehyde-3-phosphate dehydrogenase; HOTTIP: HOXA transcript at the distal tip; lnc: long non-coding; miR: microRNA; MPP^+: 1-methyl-4-phenylpyridium; NS: not significant.

We also measured the number of TH-labeled neurons and Caspase-3-labeled apoptotic neurons in the SN area. TH-positive cells and TH expression were decreased, whereas Caspase-3-positive cells and Caspase-3 and Bax expressions were increased in PD mice compared with sham mice (**Figure 7E–H**). Furthermore, HPLC was performed to evaluate dopamine content in the striatal area. Dopamine content was reduced in the MPTP-treated mice compared with sham mice, and HOTTIP knockdown enhanced the dopamine level significantly (**Figure 7I**). These results suggest that HOTTIP knockdown exerted a neuroprotective effect in PD mice.

HOTTIP knockdown suppresses neuroinflammation and microglial activation in PD mice

We used immunohistochemistry and western blot to examine microglial activation in the SN area. The number of Iba1-positive cells and Iba1 expression were increased in PD mice compared with sham mice (**Figure 8A** and **B**). In contrast, the Iba1-positive cell number and Iba1 expression were both decreased in HOTTIP knockdown PD mice compared with control PD mice (**Figure 8A** and **B**).

In addition, the expression of inflammatory cytokines and proteins was measured in the SN area. IL-lβ, IL-6, IL-18, TNF-α, iNOS, COX2, and phosphorylated NF-κB were upregulated in the PD group compared with the sham group, and the increased expression of these factors was ameliorated in the HOTTIP knockdown PD group compared with the MPTP + sh-NC group ($P < 0.05$; **Figure 8C–E**). Furthermore, HOTTIP knockdown alleviated MPTP-induced NLRP3-ASC-Caspase-1 inflammasome activation ($P < 0.05$; **Figure 8F**). In the SN area, HOTTIP levels were increased, whereas miR-615-3p and FOXO1 levels were decreased in the MPTP group compared with the sham group ($P < 0.001$; **Figure 8G–I**). HOTTIP was downregulated, whereas miR-615-3p and FOXO1 were upregulated in HOTTIP knockdown PD mice compared with control PD mice ($P < 0.001$; **Figure 8G–I**). The above results suggested that the downregulation of HOTTIP alleviated neuroinflammation in the PD model by regulating miR-615-3p and FOXO1.

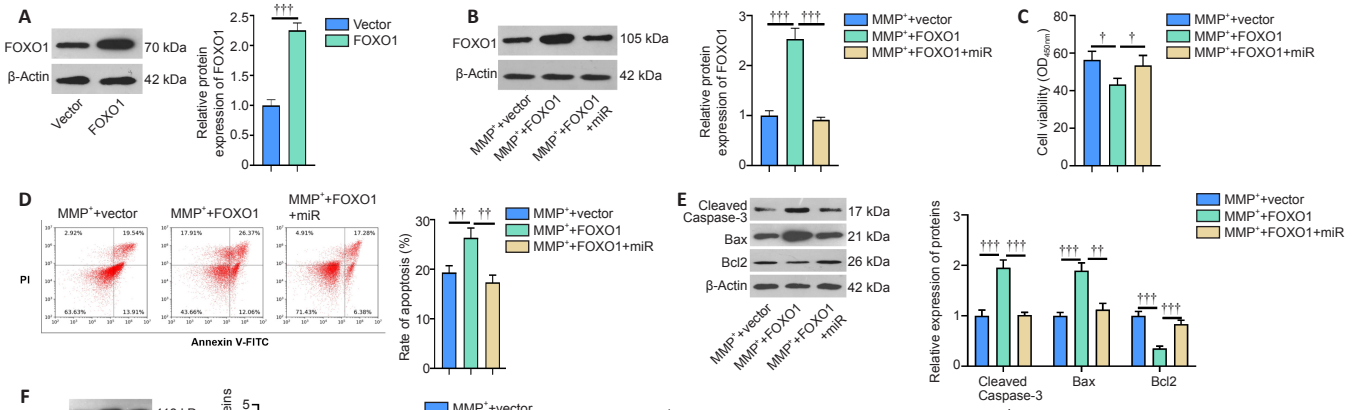

Figure 5 | FOXO1 overexpression exacerbates MPP$^+$-induced neuronal damage in SH-SY5Y cells.
(A) A FOXO1 overexpression cell model was constructed in SH-SY5Y cells, and FOXO1 protein expression was measured by western blot. (B) Cells overexpressing FOXO1 were transfected with miR-615-3p and treated with MPP$^+$ (100 μM) for 24 hours, and then FOXO1 protein expression (fold to vector) was measured by western blot. (C) Cell Counting Kit-8 was implemented to assess cell viability. (D) Flow cytometry was conducted to assess apoptosis. (E, F) Western blot was used to measure the levels (fold to MMP$^+$ vector) of apoptosis-related proteins (Caspase-3, Bax, and Bcl2) and NLRP3-ASC-Caspase-1 inflammasome. Data are expressed as mean ± SD. The experiment was repeated three times. ††$P < 0.01$, †††$P < 0.001$ (Student's *t*-test). ASC: Adaptor protein apoptosis-associated speck-like protein containing CARD domain; FOXO1: Forkhead box protein O1; miR: microRNA; MPP$^+$: 1-methyl-4-phenylpyridium; NLRP3: NLR family pyrin domain containing 3; NS: not significant.

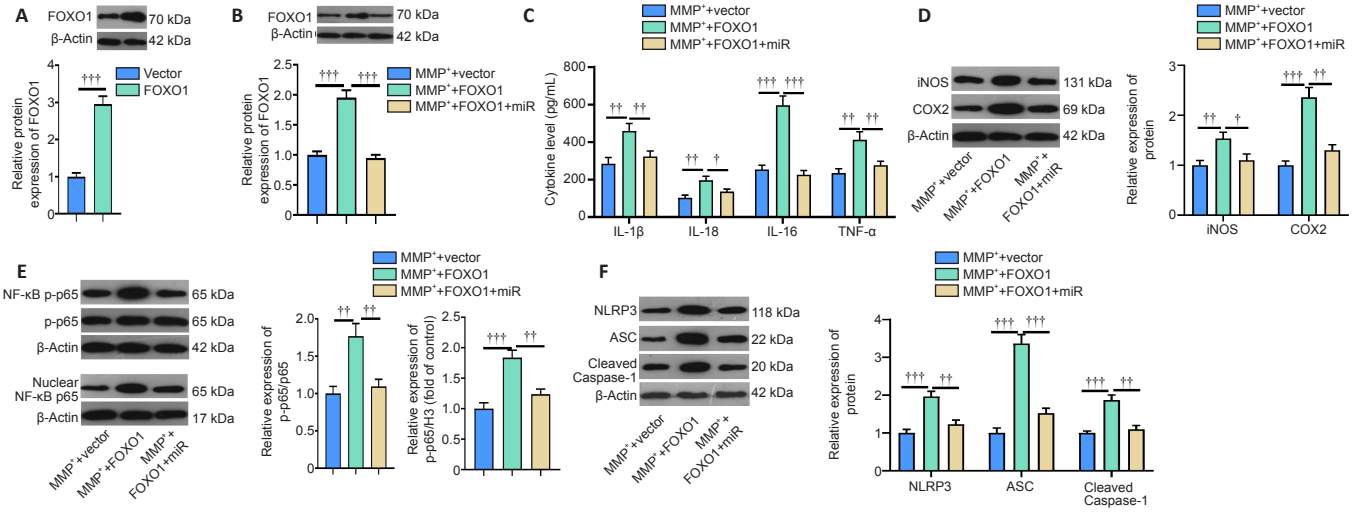

Figure 6 | FOXO1 enhances the role of MPP$^+$-induced inflammation in microglia (BV2 cells).
(A) A FOXO1 overexpression cell model was constructed in BV2 cells, and the FOXO1 protein level (fold to vector) was measured by western blot. (B) BV2 cells overexpressing FOXO1 were transfected with miR-615-3p and treated with MPP$^+$ (100 μM) for 24 hours. FOXO1 protein expression (fold to MMP$^+$ vector) was measured by western blot. (C) IL-lβ, IL-6, IL-18, and TNF-α levels produced by BV2 cells were measured by ELISA. (D–F) Western blot was used to measure the activation of the pro-oxidant proteins iNOS and COX2 (D), proinflammatory protein phosphorylated NF-κB (E), and NLRP3-ASC-cleaved Caspase-1 inflammasome (F) (fold to control). Data are expressed as mean ± SD. The experiment was repeated three times. †$P < 0.05$, ††$P < 0.01$, †††$P < 0.001$ (Student's *t*-test). ASC: Adaptor protein apoptosis-associated speck-like protein containing CARD domain; COX2: cyclooxygenase-2; ELISA: enzyme linked immunosorbent assay; FOXO1: Forkhead box protein O1; IL: interleukin; iNOS: inducible nitric oxide synthase; MPP$^+$: 1-methyl-4-phenylpyridium; NLRP3: NLR family pyrin domain containing 3; TNF-α: tumor necrosis factor-α.

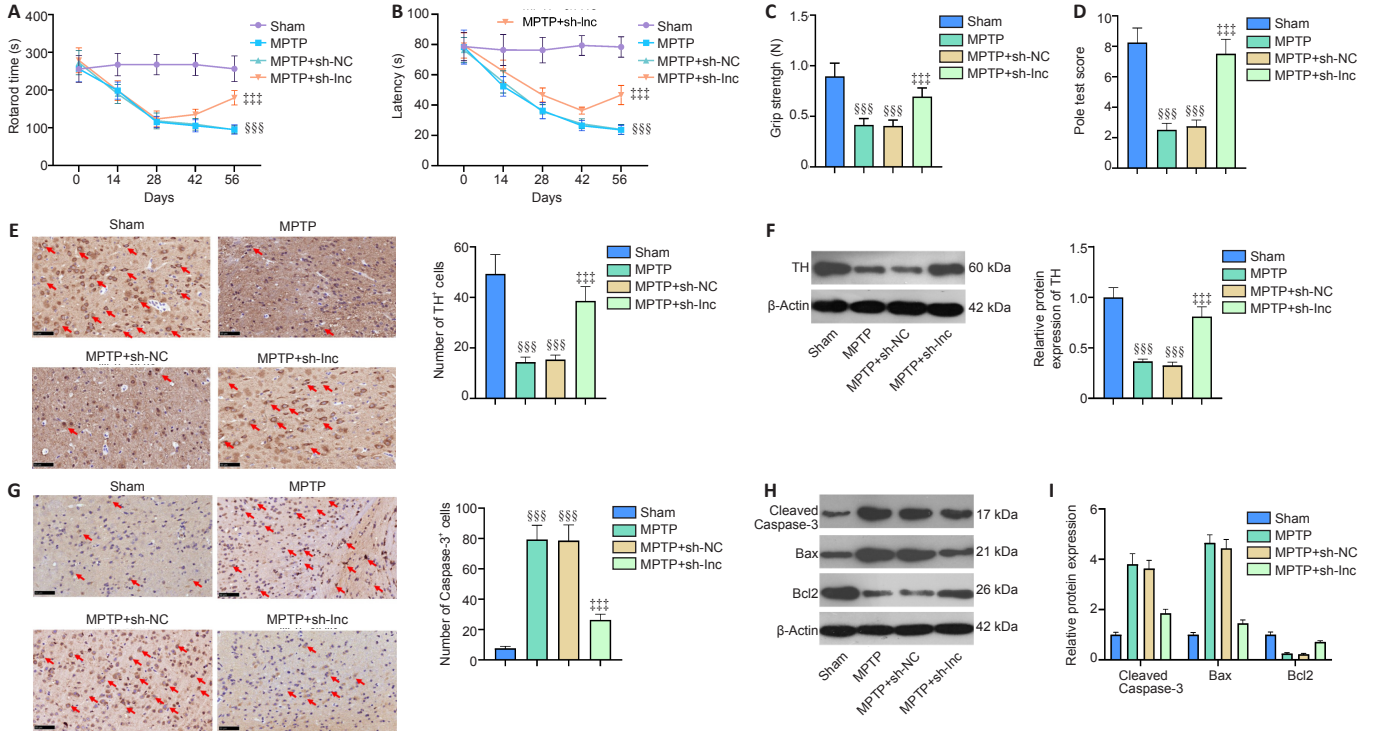

Figure 7 | **HOTTIP knockdown alleviated neurological dysfunction and neuronal damage in PD mice.**
MPTP was used to induce a PD mouse model. Sh-HOTTIP was used to knock down HOTTIP in the PD mouse model. (A) Rotarod test was conducted to evaluate motor function. (B, C) Muscular forelimb strength was examined by latency to fall and grip strength. (D) The pole test was used to examine bradykinesia. (E, F) Immunohistochemistry and western blot were used to examine TH-labeled neurons and TH protein expression (fold to sham) in the substantia nigra area. TH-positive cells were reduced in the MPTP and MPTP + sh-NC groups compared with the sham group. HOTTIP knockdown increased TH-positive cells in PD mice. (G) Immunohistochemistry was conducted to measure the number of Caspase-3-labeled apoptotic neurons. (H) Cleaved Caspase-3, Bax, and Bcl2 expression (fold to sham) in substantia nigra was measured by western blot. (I) High performance liquid chromatography was performed to measure dopamine content in the striatal area. Data are expressed as mean ± SD (n = 5). §§§P < 0.001, *vs.* sham group; ‡‡‡P < 0.001, *vs.* MPTP + sh-NC group (Student's t-test). HOTTIP: HOXA transcript at the distal tip; MPTP: 1-methyl-4-phenyl-1,2,3,6-tetrahydropyridine; PD: Parkinson's disease; TH: tyrosine hydroxylase.

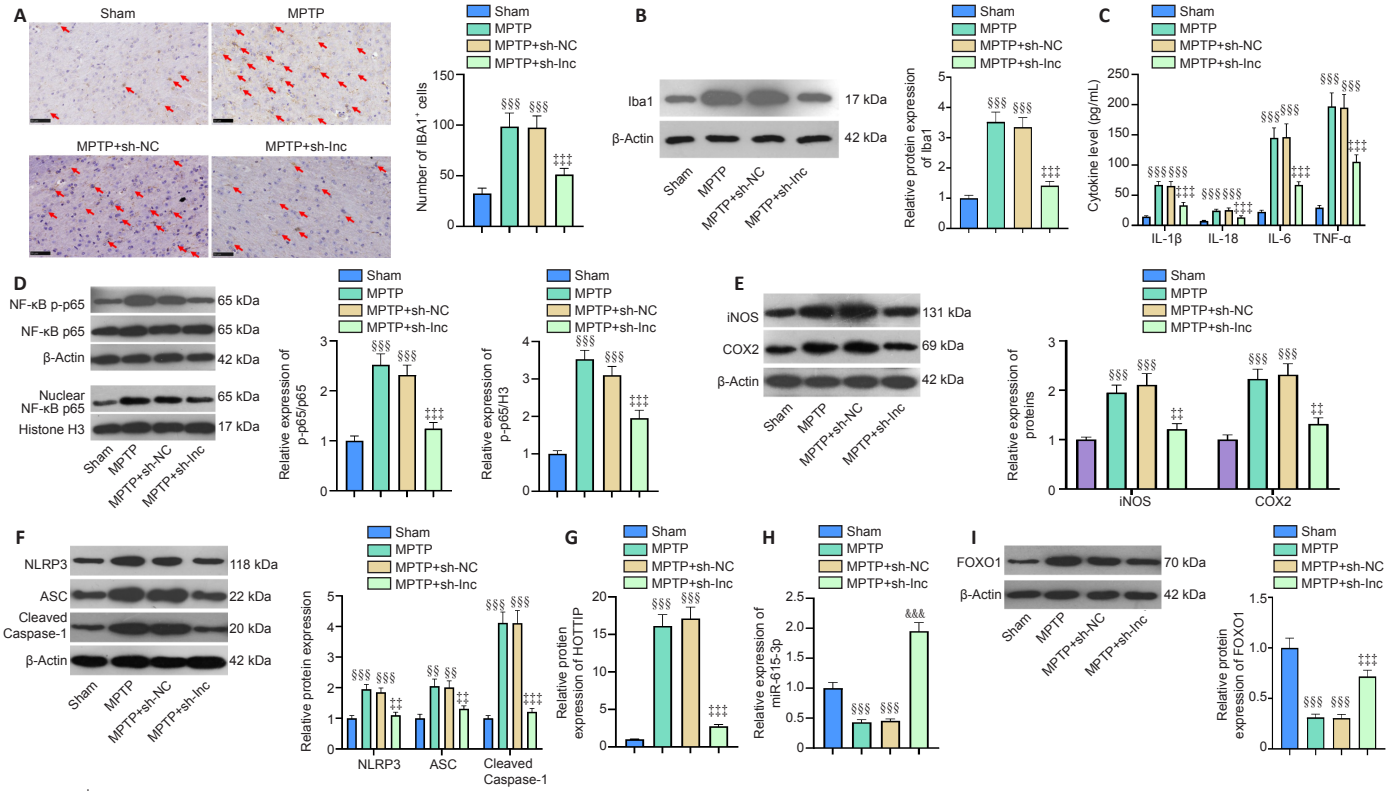

Figure 8 | **HOTTIP knockdown suppresses neuroinflammation and microglial activation in PD mice.**
(A, B) Microglial activation (labeled by Iba1) in the substantia nigra area was measured by immunohistochemistry and western blot (fold to sham). TH-positive cells were increased in the MPTP and MPTP + sh-NC groups compared with the sham group. HOTTIP knockdown reduced TH-positive cells in PD mice. (C) ELISA was used to measure IL-lβ, IL-6, IL-18, and TNF-α levels in the substantia nigra area of PD mice. (D–F) Western blot was used to measure the expression (fold to sham) of pro-oxidant proteins iNOS and COX2, proinflammatory protein phosphorylated NF-κB, and NLRP3-ASC-cleaved Caspase-1 inflammasome. (G, H) Reverse transcription-polymerase chain reaction was used to measure HOTTIP (G) and miR-615-3p (H) levels (fold to sham) in the substantia nigra area. (I) Western blot was used to measure the FOXO1 level (fold to sham) in the substantia nigra area. Data are expressed as mean ± SD (n = 5). §§P < 0.01, §§§P < 0.001, *vs.* sham group; ‡‡P < 0.01, ‡‡‡P < 0.001, *vs.* MPTP + sh-NC group (Student's t-test). ASC: adaptor protein apoptosis-associated speck-like protein containing CARD domain; COX2: cyclooxygenase-2; ELISA: enzyme linked immunosorbent assay; FOXO1: Forkhead box protein O1; HOTTIP: HOXA transcript at the distal tip; Iba1: induction of brown adipocytes 1; IL: interleukin; iNOS: inducible nitric oxide synthase; NF-κB: nuclear factor kappa B; NLRP3: NLR family pyrin domain containing 3; PD: Parkinson's disease; TNF-α: tumor necrosis factor-α.

Discussion

PD is a common neurodegenerative disorder and the most frequent extrapyramidal disease in middle-aged and older people. Over the years, several studies have reported that neuroinflammation, neuronal excitotoxicity, genetic mutations and incorrect protein folding are important factors in PD pathophysiology (Liu et al., 2021). Here, we probed the molecular mechanism of the HOTTIP/miR-615-3p/FOXO1 axis in PD. Our results suggest that HOTTIP mediates neuronal apoptosis and microglial activation through the miR-615-3p/FOXO1 axis to produce excessive proinflammatory responses, thereby exacerbating neuronal damage.

Noncoding RNAs have an important role in brain development, and have distinct expression in the brain (Schaukowitch and Kim, 2014). In particular, lncRNAs play an important role in CNS inflammatory response regulation. For example, lncRNA MALAT1 shuttled by exosomes from adipose-derived stem cells not only reduces traumatic brain injury-induced neurological damage, but also attenuates inflammation pathways (Patel et al., 2018). Additionally, lncRNA colorectal neoplasia differentially expressed (CRNDE) is upregulated in the plasma of traumatic brain injury patients and mice, and inhibiting CRNDE alleviates traumatic brain injury-mediated neurological dysfunction and reduces neuroinflammatory factor expression and neuronal damage (Yi et al., 2019). Moreover, lncRNAs can regulate microglial inflammation in CNS diseases. For example, lncRNA metastasis suppressor-1 (Mtss1) is upregulated in brain lesions after intracerebral hemorrhage, and it inhibits TIR-domain-containing adapter-inducing interferon-β expression, P65 phosphorylation, TNF-α and IL-1β secretion, and microglial activation (Chen et al., 2020a). Furthermore, lncRNA small nucleolar RNA host gene 5 is significantly upregulated in a mouse spinal nerve ligation model, and its inhibition eases nerve pain through miR-154-5p/CXCL13 and alleviates neuroinflammation caused by microglial and astrocyte activation (Chen et al., 2020c). These studies support the prominent function of lncRNAs in regulating CNS inflammation. Similarly, lncRNA HOTTIP also contributes to inflammatory diseases such as rheumatoid arthritis (Hu et al., 2020) and inflammation mediated by high glucose (Zhu et al., 2019). These studies indicate that HOTTIP has a proinflammatory function.

Here, we found that HOTTIP was upregulated in MPP^+- and MPTP-induced PD models, both *in vitro* and *in vivo*. HOTTIP overexpression facilitated MPP^+-treated nerve cell damage and microglial inflammation, and HOTTIP knockdown attenuated the neurological damage in PD model mice and suppressed DAN apoptosis and microglial activation in the SN area. These results indicate that HOTTIP inhibition has anti-inflammatory and neuroprotective effects. Moreover, HOTTIP knockdown significantly increased the dopamine level in the striatal area compared with that in the negative control group. Hence, we consider that HOTTIP downregulation also improves striatal dopaminergic projections in the PD mouse model.

Multiple studies have confirmed that abnormal miRNA expression modulates neuronal apoptosis and microglial activation. For example, miR-188-5p attenuates oxygen-glucose deprivation-mediated neuronal damage and inhibits PTEN expression (Li et al., 2020a). Additionally, miR-216a suppresses SH-SY5Y cell death by targeting Bax in MPP^+-induced PD models *in vitro* (Yang et al., 2020). Similarly, miR-29c and miR-190 can also reduce neuronal apoptosis and microglial inflammation in MPTP-treated mice and MPP^+-treated SH-SY5Y cells (Sun et al., 2019; Wang et al., 2020). These studies indicate that miRNAs have extensive regulatory effects in CNS diseases. In this study, we confirmed through *in vitro* experiments that miR-615-3p attenuates MPP^+-induced neuronal damage and microglial activation, suggesting that miR-615-3p has a neuroprotective effect in PD. Furthermore, previous studies have shown that HOTTIP regulates the progression of gastric cancer (Xiao et al., 2020) and renal cell carcinoma (Wang et al., 2018a) by modulating miR-615-3p. Here, we showed that HOTTIP is an upstream regulatory gene of miR-615-3p, and that HOTTIP overexpression decreases miR-615-3p. Furthermore, miR-615-3p overexpression attenuated the neurotoxic and proinflammatory effects mediated by HOTTIP overexpression.

Multiple members of the FOXO family have been shown to regulate inflammation. For example, FOXO3 inhibition dramatically inhibits the expression of inflammatory factors in a subarachnoid hemorrhage rat model (Zuo et al., 2019). FOXO3 is upregulated in Staphylococcal enterotoxin B-mediated acute lung injury, and the inhibition of FOXO3 expression via miR-222 suppresses the Staphylococcal enterotoxin B-induced proinflammatory response and apoptosis (Chen et al., 2020b). In contrast, ε-viniferin upregulates SIRT3 expression in PD, which promotes FOXO3 deacetylation and nuclear localization, thus exerting a neuroprotective effect (Zhang et al., 2020). Moreover, inhibition of FOXO4 via adiponectin markedly attenuates NLRP3-inflammasome-mediated pyroptosis of aortic endothelial cells (Zhang et al., 2019a). Presently, we found that FOXO1 is upregulated in the PD model, and *in vitro* experiments demonstrated that FOXO1 overexpression exacerbated MPP^+-induced neuronal apoptosis and microglial activation. It has been shown that miR-135b alleviates apoptosis in MPP^+-treated SH-SY5Y and PC-12 PD model cells; mechanically, miR-135b targets and inhibits the expression of FOXO1 and inactivates NLRP3 inflammasomes (Zeng et al., 2019). Previous studies have demonstrated that miR-615-3p targets FOXO1 (Yin et al., 2017), which was also confirmed in the present study. Our results showed that miR-615-3p overexpression weakened the effect of FOXO1 overexpression.

NLRP3 inflammasomes are multiprotein complexes assembled by NLRP3 (also called NALP3 or cryopyrin), cysteinyl aspartate-specific protease (caspase-1) precursor and apoptosis-associated speck-like protein containing CARD (ASC), and are important parts of the natural immune system (Li et al., 2020b). After being affected by pathogen-associated molecular patterns or host-derived damage-associated molecular patterns, NLRP3 recruits and activates protease caspase-1, which accelerates the release of IL-1β and IL-18 and induces inflammation (Liu et al., 2020b). Recently, researchers have shown that NLRP3 inflammasome activation is related to the occurrence and progression of Alzheimer's disease and amyotrophic lateral sclerosis (Söderbom and Zeng, 2020). Importantly, NLRP3 inflammasome activation is associated with the PD pathogenesis; after NLRP3 activation in microglia, proinflammatory cytokines are produced, which directly mediates neuronal damage (Wang et al., 2019; Haque et al., 2020). Also, NLRP3 inflammasome is increased in mesencephalic neurons of PD patients, and DAN is a cellular source of inflammasome activity, suggesting that inflammasome activity influences PD development (von Herrmann et al., 2018). In this study, we showed that the upregulation of HOTTIP and FOXO1 induced NLRP3 inflammasome activation, which is consistent with their proinflammatory and nerve damaging effects reported in previous studies. In contrast, miR-615-3p inhibited the apoptosis and microglial damage of MPP^+-treated SH-SY5Y cells and offset the effects caused by HOTTIP and FOXO1 upregulation.

Overall, this study showed that HOTTIP and FOXO1 exacerbate neuronal damage and microglial inflammation in PD models *in vivo* and *in vitro*. Our findings suggest that HOTTIP dampens

miR-615-3p as a competitive endogenous RNA, upregulates FOXO1 and activates the NLRP3 inflammasome. However, several limitations of this study need to be addressed in future studies: 1) The clinical significance of the HOTTIP/miR-615-3p/FOXO1 axis in PD patients needs to be determined; 2) the regulatory axis of HOTTIP/miR-615-3p/FOXO1 should be confirmed in additional animals, including female rats; and 3) more experiments are needed to verify the upstream molecular mechanism of HOTTIP and the mechanism of the interaction between FOXO1 and NLRP3 inflammasomes.

Author contributions: *Guarantor of integrity of the entire study: PL, TJ; study conception: DHW; study design: PS; experimental and clinical studies: XL; data analysis and acquisition: XDC; manuscript preparation: PL; manuscript editing and review: SY. All authors read and approved the final manuscript.*
Conflicts of interest: *The authors declare that they have no conflict of interests.*
Financial support: *None.*
Institutional review board statement: *This study was approved by the Ethics Review Board of the Affiliated Hospital of Qingdao University (approval No. UDX-2018-042) in June 2018.*

Data sharing statement: *Datasets analyzed during the current study are available from the corresponding author on reasonable request.*
Plagiarism check: *Checked twice by iThenticate.*
Peer review: *Externally peer reviewed.*

Open peer reviewer: *Ariadna Laguna, Vall d'Hebron Research Institute, Spain.*
Additional file: *Open peer review report 1.*

References

Brites D, Fernandes A (2015) Neuroinflammation and depression: microglia activation, extracellular microvesicles and microrna dysregulation. Front Cell Neurosci 9:476.

Charles Richard JL, Eichhorn PJA (2018) Platforms for investigating lncRNA functions. SLAS Technol 23:493-506.

Chen JX, Wang YP, Zhang X, Li GX, Zheng K, Duan CZ (2020a) lncRNA Mtss1 promotes inflammatory responses and secondary brain injury after intracerebral hemorrhage by targeting miR-709 in mice. Brain Res Bull 162:20-29.

Chen L, Chen J, Xie G, Zhu L (2020b) MiR-222 inhibition alleviates Staphylococcal Enterotoxin B-induced inflammatory acute lung injury by targeting Foxo3. J Biosci 45:65.

Chen L, Gao B, Zhang Y, Lu H, Li X, Pan L, Yin L, Zhi X (2019) PAR2 promotes M1 macrophage polarization and inflammation via FOXO1 pathway. J Cell Biochem 120:9799-9809.

Chen M, Yang Y, Zhang W, Li X, Wu J, Zou X, Zeng X (2020c) Long noncoding RNA SNHG5 knockdown alleviates neuropathic pain by targeting the miR-154-5p/CXCL13 axis. Neurochem Res 45:1566-1575.

Frank-Cannon TC, Alto LT, McAlpine FE, Tansey MG (2009) Does neuroinflammation fan the flame in neurodegenerative diseases? Mol Neurodegener 4:47.

Guo Y, Wei X, Yan H, Qin Y, Yan S, Liu J, Zhao Y, Jiang F, Lou H (2019) TREM2 deficiency aggravates α-synuclein-induced neurodegeneration and neuroinflammation in Parkinson's disease models. FASEB J 33:12164-12174.

Haque ME, Akther M, Jakaria M, Kim IS, Azam S, Choi DK (2020) Targeting the microglial NLRP3 inflammasome and its role in Parkinson's disease. Mov Disord 35:20-33.

Hoss AG, Kartha VK, Dong X, Latourelle JC, Dumitriu A, Hadzi TC, Macdonald ME, Gusella JF, Akbarian S, Chen JF, Weng Z, Myers RH (2014) MicroRNAs located in the Hox gene clusters are implicated in huntington's disease pathogenesis. PLoS Genet 10:e1004188.

Hu X, Tang J, Hu X, Bao P, Deng W, Wu J, Liang Y, Chen Z, Gao L, Tang Y (2020) Silencing of long non-coding RNA HOTTIP reduces inflammation in rheumatoid arthritis by demethylation of SFRP1. Mol Ther Nucleic Acids 19:468-481.

Karthikeyan A, Patnala R, Jadhav SP, Eng-Ang L, Dheen ST (2016) MicroRNAs: key players in microglia and astrocyte mediated inflammation in CNS pathologies. Curr Med Chem 23:3528-3546.

Lee YY, Park JS, Leem YH, Park JE, Kim DY, Choi YH, Park EM, Kang JL, Kim HS (2019) The phosphodiesterase 10 inhibitor papaverine exerts anti-inflammatory and neuroprotective effects via the PKA signaling pathway in neuroinflammation and Parkinson's disease mouse models. J Neuroinflammation 16:246.

Li L, Cui P, Ge H, Shi Y, Wu X, Fan Ru Z (2020a) miR-188-5p inhibits apoptosis of neuronal cells during oxygen-glucose deprivation (OGD)-induced stroke by suppressing PTEN. Exp Mol Pathol 116:104512.

Li Z, Guo J, Bi L (2020b) Role of the NLRP3 inflammasome in autoimmune diseases. Biomed Pharmacother 130:110542.

Lin Q, Hou S, Dai Y, Jiang N, Lin Y (2019) LncRNA HOTAIR targets miR-126-5p to promote the progression of Parkinson's disease through RAB3IP. Biol Chem 400:1217-1228.

Liu X, Zhu N, Zhang B, Xu SB (2020a) Long noncoding RNA TCONS_00016406 attenuates lipopolysaccharide-induced acute kidney injury by regulating the miR-687/PTEN pathway. Front Physiol 11:622.

Liu Y, Dai Y, Li Q, Chen C, Chen H, Song Y, Hua F, Zhang Z (2020b) Beta-amyloid activates NLRP3 inflammasome via TLR4 in mouse microglia. Neurosci Lett 736:135279.

Liu Z, Ye Q, Wang F, Guo Y, Cui R, Wang J, Wang D (2021) Overexpression of thioredoxin reductase 1 can reduce DNA damage, mitochondrial autophagy and endoplasmic reticulum stress in Parkinson's disease. Exp Brain Res 239:475-490.

Luo D, Zhao J, Cheng Y, Lee SM, Rong J (2018) N-propargyl caffeamide (PACA) ameliorates dopaminergic neuronal loss and motor dysfunctions in MPTP mouse model of Parkinson's disease and in MPP(+)-induced neurons via promoting the conversion of proNGF to NGF. Mol Neurobiol 55:2258-2267.

Neal M, Richardson JR (2018) Epigenetic regulation of astrocyte function in neuroinflammation and neurodegeneration. Biochim Biophys Acta Mol Basis Dis 1864:432-443.

Patel NA, Moss LD, Lee JY, Tajiri N, Acosta S, Hudson C, Parag S, Cooper DR, Borlongan CV, Bickford PC (2018) Long noncoding RNA MALAT1 in exosomes drives regenerative function and modulates inflammation-linked networks following traumatic brain injury. J Neuroinflammation 15:204.

Paxinos G, Watson C (2007) The rat brain in stereotaxic coordinates, 6th ed. Cambridge, USA: Academic Press/Elsevier.

Prasad KN (2017) Oxidative stress, pro-inflammatory cytokines, and antioxidants regulate expression levels of microRNAs in Parkinson's disease. Curr Aging Sci 10:177-184.

Pu HY, Xu R, Zhang MY, Yuan LJ, Hu JY, Huang GL, Wang HY (2017) Identification of microRNA-615-3p as a novel tumor suppressor in non-small cell lung cancer. Oncol Lett 13:2403-2410.

Rocha EM, De Miranda B, Sanders LH (2018) Alpha-synuclein: Pathology, mitochondrial dysfunction and neuroinflammation in Parkinson's disease. Neurobiol Dis 109:249-257.

Rudd MD, Gonzalez-Robayna I, Hernandez-Gonzalez I, Weigel NL, Bingman WE 3rd, Richards JS (2007) Constitutively active FOXO1a and a DNA-binding domain mutant exhibit distinct co-regulatory functions to enhance progesterone receptor A activity. J Mol Endocrinol 38:673-690.

Schaukowitch K, Kim TK (2014) Emerging epigenetic mechanisms of long non-coding RNAs. Neuroscience 264:25-38.

Schneider RB, Iourinets J, Richard IH (2017) Parkinson's disease psychosis: presentation, diagnosis and management. Neurodegener Dis Manag 7:365-376.

Singh S, Jamwal S, Kumar P (2017) Neuroprotective potential of Quercetin in combination with piperine against 1-methyl-4-phenyl-1,2,3,6-tetrahydropyridine-induced neurotoxicity. Neural Regen Res 12:1137-1144.

Söderbom G, Zeng BY (2020) The NLRP3 inflammasome as a bridge between neuro-inflammation in metabolic and neurodegenerative diseases. Int Rev Neurobiol 154:345-391.

Sun Q, Wang S, Chen J, Cai H, Huang W, Zhang Y, Wang L, Xing Y (2019) MicroRNA-190 alleviates neuronal damage and inhibits neuroinflammation via Nlrp3 in MPTP-induced Parkinson's disease mouse model. J Cell Physiol 234:23379-23387.

Surmeier DJ (2018) Determinants of dopaminergic neuron loss in Parkinson's disease. FEBS J 285:3657-3668.

Vivekanantham S, Shah S, Dewji R, Dewji A, Khatri C, Ologunde R (2015) Neuroinflammation in Parkinson's disease: role in neurodegeneration and tissue repair. Int J Neurosci 125:717-725.

von Herrmann KM, Salas LA, Martinez EM, Young AL, Howard JM, Feldman MS, Christensen BC, Wilkins OM, Lee SL, Hickey WF, Havrda MC (2018) NLRP3 expression in mesencephalic neurons and characterization of a rare NLRP3 polymorphism associated with decreased risk of Parkinson's disease. NPJ Parkinsons Dis 4:24.

Wakabayashi K, Tanji K, Odagiri S, Miki Y, Mori F, Takahashi H (2013) The Lewy body in Parkinson's disease and related neurodegenerative disorders. Mol Neurobiol 47:495-508.

Wang LQ, Zhou HJ (2018) LncRNA MALAT1 promotes high glucose-induced inflammatory response of microglial cells via provoking MyD88/IRAK1/TRAF6 signaling. Sci Rep 8:8346.

Wang Q, Wu G, Zhang Z, Tang Q, Zheng W, Chen X, Chen F, Li Q, Che X (2018a) Long non-coding RNA HOTTIP promotes renal cell carcinoma progression through the regulation of the miR-615/IGF-2 pathway. Int J Oncol 53:2278-2288.

Wang R, Yang Y, Wang H, He Y, Li C (2020) MiR-29c protects against inflammation and apoptosis in Parkinson's disease model in vivo and in vitro by targeting SP1. Clin Exp Pharmacol Physiol 47:372-382.

Wang S, Yuan YH, Chen NH, Wang HB (2019) The mechanisms of NLRP3 inflammasome/pyroptosis activation and their role in Parkinson's disease. Int Immunopharmacol 67:458-464.

Wang Y, Li G, Zhao L, Lv J (2018b) Long noncoding RNA HOTTIP alleviates oxygen-glucose deprivation-induced neuronal injury via modulating miR-143/hexokinase 2 pathway. J Cell Biochem 119:10107-10117.

Xiao ZS, Long H, Zhao L, Li HX, Zhang XN (2020) LncRNA HOTTIP promotes proliferation and inhibits apoptosis of gastric carcinoma cells via adsorbing miR-615-3p. Eur Rev Med Pharmacol Sci 24:6692-6698.

Xing YQ, Li A, Yang Y, Li XX, Zhang LN, Guo HC (2018) The regulation of FOXO1 and its role in disease progression. Life Sci 193:124-131.

Xiong XY, Liu L, Yang QW (2016) Functions and mechanisms of microglia/macrophages in neuroinflammation and neurogenesis after stroke. Prog Neurobiol 142:23-44.

Xu W, Zhang L, Geng Y, Liu Y, Zhang N (2020) Long noncoding RNA GAS5 promotes microglial inflammatory response in Parkinson's disease by regulating NLRP3 pathway through sponging miR-223-3p. Int Immunopharmacol 85:106614.

Yang M, Wei Y, Jiang F, Wang Y, Guo X, He J, Kang L (2014) MicroRNA-133 inhibits behavioral aggregation by controlling dopamine synthesis in locusts. PLoS Genet 10:e1004206.

Yang X, Zhang M, Wei M, Wang A, Deng Y, Cao H (2020) MicroRNA-216a inhibits neuronal apoptosis in a cellular Parkinson's disease model by targeting Bax. Metab Brain Dis 35:627-635.

Yi M, Dai X, Li Q, Xu X, Chen Y, Wang D (2019) Downregulated lncRNA CRNDE contributes to the enhancement of nerve repair after traumatic brain injury in rats. Cell Cycle 18:2332-2343.

Yin J, Zhuang G, Zhu Y, Hu X, Zhao H, Zhang R, Guo H, Fan X, Cao Y (2017) MiR-615-3p inhibits the osteogenic differentiation of human lumbar ligamentum flavum cells via suppression of osteogenic regulators GDF5 and FOXO1. Cell Biol Int 41:779-786.

Zeng R, Luo DX, Li HP, Zhang QS, Lei SS, Chen JH (2019) MicroRNA-135b alleviates MPP(+)-mediated Parkinson's disease in in vitro model through suppressing FoxO1-induced NLRP3 inflammasome and pyroptosis. J Clin Neurosci 65:125-133.

Zhang L, Yuan M, Zhang L, Wu B, Sun X (2019a) Adiponectin alleviates NLRP3-inflammasome-mediated pyroptosis of aortic endothelial cells by inhibiting FoxO4 in arteriosclerosis. Biochem Biophys Res Commun 514:266-272.

Zhang S, Ma Y, Feng J (2020) Neuroprotective mechanisms of ε-viniferin in a rotenone-induced cell model of Parkinson's disease: significance of SIRT3-mediated FOXO3 deacetylation. Neural Regen Res 15:2143-2153.

Zhang X, Zhu XL, Ji BY, Cao X, Yu LJ, Zhang Y, Bao XY, Xu Y, Jin JL (2019b) LncRNA-1810034E14Rik reduces microglia activation in experimental ischemic stroke. J Neuroinflammation 16:75.

Zhong L, Simard MJ, Huot J (2018) Endothelial microRNAs regulating the NF-κB pathway and cell adhesion molecules during inflammation. FASEB J 32:4070-4084.

Zhu XJ, Gong Z, Li SJ, Jia HP, Li DL (2019) Long non-coding RNA Hottip modulates high-glucose-induced inflammation and ECM accumulation through miR-455-3p/WNT2B in mouse mesangial cells. Int J Clin Exp Pathol 12:2435-2445.

Zuo Y, Huang L, Enkhjargal B, Xu W, Umut O, Travis ZD, Zhang G, Tang J, Liu F, Zhang JH (2019) Activation of retinoid X receptor by bexarotene attenuates neuroinflammation via PPARγ/SIRT6/FoxO3a pathway after subarachnoid hemorrhage in rats. J Neuroinflammation 16:47.

P-Reviewer: Laguna A; C-Editor: Zhao M; S-Editors: Yu J, Li CH; L-Editors: McCollum L, Yu J, Song LP; T-Editor: Jia Y